Effects of Ammonia on the Pyrolytic Decomposition of Alkylaluminum Amides to Aluminum Nitride

Frederick C. Sauls*

Department of Chemistry, King's College, Wilkes-Barre, Pennsylvania 18711

William J. Hurley, Jr.† and Leonard V. Interrante*

Department of Chemistry, Rensselaer Polytechnic Institute, Troy, New York 12180-3590

Paul S. Marchetti and Gary E. Maciel

Department of Chemistry, Colorado State University, Fort Collins, Colorado 80523

Received February 7, 1995. Revised Manuscript Received April 17, 1995®

The thermal decomposition of the organoaluminum amides, $[R_2AlNH_2]_3$, R = Et and Me, to form AlN and 2RH, have been studied by NMR, IR, TGA, DSC, and other methods. Kinetic studies of the initial stages of the decomposition of the R = Me compound, both in solution and in the condensed phase, indicate a first-order process with an activation energy of 123 ± 11 kJ/mol. The addition of ammonia is found, qualitatively, to markedly increase the rate of decomposition of these amides, while leading to more complete elimination of the hydrocarbon, RH. It also yields, at higher temperatures, an AlN product of higher purity (lower carbon content) and improved crystallinity. A mechanism is proposed for the first and second stages of this decomposition in the absence of ammonia. In the first stage (amide → imide + RH), the heterolytic opening of the $(AlN)_3$ rings of the amide is postulated as the rate-determining step, which is followed by attack of the terminal nitrogen on a second $(AlN)_3$ ring, leading, eventually, to higher oligomeric species. It is postulated that ammonia increases the rate of decomposition by providing a more facile pathway for ring opening (though direct nucleophilic attack on the Al centers); the resultant open-chain species is then stabilized by adduct formation with the NH_3. In addition to increasing the rate of decomposition, the added NH_3 can then serve as an additional source of H for RH elimination, thus leading to the more complete elimination of the hydrocarbon and a lower C content in the AlN final product.

Introduction

The generation of non-oxide ceramics by pyrolysis of a suitable organometallic precursor has been widely pursued as a general route to ceramic fibers, coatings, matrices, etc., as well as binders, joining aids, and powder sources for monolithic ceramics.[1] While much progress has been made in developing this approach, the mechanisms of the underlying thermal elimination reactions and structural rearrangements have not been widely studied. These processes are important to understanding the chemistry of the organometallics involved, as well as for the practical goal of an improved product.

Aluminum nitride is a ceramic with attractive properties for electronic, optical, and structural applications.[2-13] It is generally made from the oxide, by carbothermal reduction[14,15] or from the metal by direct reaction with N_2. These are both high-temperature processes which cannot be used to produce AlN in the final form (e.g., thin epitaxial films or protective coatings) needed for certain applications. The use of a volatile or organo-soluble precursor might enable preparation of the desired final form directly by a CVD or solution casting/pyrolysis process as well as allowing better control of the product composition, impurity content, and microstructure.[1] Among the organometallic precursor systems that have been employed to generate thin films by CVD[16] is the organoaluminum amide $[Me_2AlNH_2]_3$.[17,18] This compound can be viewed as one of the intermediates in a series of reactions which begin with the

† Present address: Foster-Miller, Inc., 350 Second Ave., Waltham, Massachusetts 02154-1196

® Abstract published in *Advance ACS Abstracts,* June 1, 1995.

(1) Baixia, L.; Yinkui, L.; Yi, L. *J. Mater. Chem.* **1993**, *3*, 117. Fischer, H. E.; Larkin, D.; Interrante, L. V. *MRS Bull.* **1991**, *April*, 59. Peuckert, M.; Vaahs, T.; Bruck, M. *Adv. Mater.* **1990**, *2*, 398. Wynne, K. J.; Rice, R. W. *Annu. Rev. Mater. Sci.* **1984**, *14*, 297.
(2) Slack, G. A.; Tanzili, R. A.; Pohl, R. O.; Vandersande, J. W. *J. Phys. Chem. Solids* **1987**, *48*, 641.
(3) Kuramato, N.; Taniguchi, H. *J. Mater. Sci. Lett.* **1984**, *3*, 471.
(4) Slack, G. A.; McNelly, T. F. *J. Cryst. Growth* **1976**, *34*, 263.
(5) Slack, G. A.; Bartram, S. F. *J. Appl. Phys.* **1975**, *46*, 89.
(6) Slack, G. A.; McNelly, T. F. *J. Cryst. Growth* **1977**, *42*, 550.
(7) Slack, G. A. *J. Phys. Chem. Solids* **1973**, *34*, 321.
(8) Fujii, Y.; Yoshida, S.; Misawa, S.; Maekawa, S.; Sakudo, T. *Appl. Phys. Lett.* **1977**, *31*, 815.
(9) Kline, G. R.; Lakin, K. M. *Proc. IEEE Symp. Ultrasonics* **1983**, 495.
(10) Kitayama, M.; Fukui, T.; Shiosaki, T.; Kawabata, A. *Jpn. J. Appl. Phys.* **1982**, *22* (Supplement), 139.
(11) Tsubouchi, K.; Sugai, K. *Mikoshiba Proc. IEEE Symp. Ultrasonics* **1983**, 340.
(12) Sano, M.; Aoki, M. *Oyo Butsuri* **1983**, *52*, 374.
(13) Norton, M. G.; Steele, B. C. H.; Leach, C. A. *Sci. Ceram.* **1988**, *14*, 545.
(14) Forslung, B.; Zheng, J. *J. Mater. Sci.* **1993**, *28*, 3125.
(15) Rabineau, A. In *Compound Semiconductors*; Willardson, R. K., Goering, H. L., Eds.; Reinhold: New York, 1962; Vol. 1, Chapter 19, p 174.

0897-4756/95/2807-1361$09.00/0

corresponding R_3Al and NH_3, i.e.

$$R_3Al + NH_3 \rightarrow R_3AlNH_3 \rightarrow \underset{\text{"adduct"}}{} (R_2AlNH_2)_n \rightarrow (RAlNH)_n \rightarrow AlN(s) \quad (1)$$
$$\text{"amide"} \qquad \text{"imide"}$$

The chemistry of some of these intermediates have been investigated and the results summarized.[19-25] In particular, the "amides" are typically cyclic oligomers of the type $[R_2AlNH_2]_n$ ($n = 2$ or 3)[21] and the "imides" exist in a wide range of ring, cage, and network polymer forms[24] depending largely on the nature of the substituent R and whether the H on the N is substituted by an organic group.

Pyrolysis of the amides or imides obtained from reaction 1 in vacuum or an inert atmosphere yields a black product high in carbon; however, pyrolysis under ammonia yields high purity AlN.[26,27]

As a beginning in understanding the processes which transform the adduct to AlN we studied the mechanism for the first step. We concluded that the loss of alkane from the adduct, R_3AlNH_3, to form the amide $(R_2AlNH_2)_2$ is catalyzed by the monomeric species R_2AlNH_2, which is in rapid equilibrium with the corresponding dimeric and trimeric species.[28,29] The immediate product of alkane loss is a dimeric amide which presumably exists in the form of a four-membered $(AlN)_2$ ring. In solution and vapor, both $(R_2AlNH_2)_2$ and $(R_2AlNH_2)_3$ (i.e., both four- and six-membered rings) are present; equilibration is catalyzed by amines which open the rings.[19,29]

In this paper we examine the loss of the second and third alkane molecules from cyclic alkylaluminum amides, recrystallization of the AlN product, and the influence of ammonia on these processes.

Experimental Section

$(Et_2AlNH_2)_3$ was prepared[27] by adding ammonia to a solution of $(Et_3Al)_2$ in hexane at 50 °C. The hexane was removed under reduced pressure at ambient temperature to yield the liquid amide. **[Caution: The solution should be warmed before and during ammonia addition to prevent possible buildup of the unstable Lewis acid–base adduct, which can decompose explosively. Also, the starting Et_3Al and the product amide are highly air and moisture sensitive and may inflame on exposure to the atmosphere].** ^{15}N-enriched $(Et_2AlNH_2)_3$ was prepared identically using 10% ^{15}N ammonia. Separate samples of both labeled and unlabeled $(Et_2AlNH_2)_3$ were heated in Mo boats under flowing NH_3 for 4 h at 200, 350, 500, 800, and 1000 °C. Samples of the 1000 °C unlabeled AlN product were heated to 1600 °C for 4 h under N_2.

To avoid reaction with H_2O or oxygen, IR samples were prepared in the glovebox. They were ground in a B_4C mortar and pestle and pressed with dry KBr powder. The resultant disks were transferred under N_2 to the Perkin-Elmer 1850 FTIR. The GC was a Shimadzu GC-9A equipped with an Alltech VZ-10 or Chromosorb 103 column (6 ft, 0.085 in., 80/100 mesh). Perkin-Elmer DSC 7 and TGA 7 instruments were used for thermal analysis. DSC was performed in sealed cells at 2 or 5 °C/min; TGA at 10 °C/min under flowing nitrogen or ammonia. Samples were loaded for TGA measurements under dry N_2 in a specially prepared glovebox enclosure around the TGA instrument.

All samples for NMR studies were prepared and loaded into NMR tubes in a N_2-filled glovebox. ^1H NMR spectra were obtained on a Varian XL-200 spectrometer. The solvent (when used) was tetrahydronaphthalene-d_{12}. Appropriate recycle delays were used to ensure quantitative results. Temperatures were determined from the peak separation in a sealed ethylene glycol sample.[30]

^{13}C CPMAS NMR spectra were obtained on a Nicolet NT-200 spectrometer at 50.289 MHz. Pulse width was 30°, contact time was 28 ms, and recycle delay was 5 s. Spin rates were 2.5–4 kHz for ^{13}C and ^{15}N spectra. Single-pulse spectra were acquired with high-power proton decoupling and a 120 s relaxation delay.

^{27}Al MAS NMR spectra were acquired using a Bruker AM-600 spectrometer at 156.38 MHz. 30° pulses were applied with 1 s delays. The spinning rate was 10–12 kHz.

^{15}N MAS spectra were acquired on a Nicolet NT-200 at 20.266 MHz. Single-pulse (30°) spectra with ^1H decoupling were acquired for the 200 °C sample, using relaxation delays 30–900 s. No improvement in the S/N was noted for times greater than 120 s. CPMAS spectra (12 ms contact time) were acquired on each sample, where significant signal enhancement by way of cross polarization from protons to ^{15}N occurs. These spectra represent ^{15}N which bear hydrogen atoms. Interrupted decoupling spectra were acquired in the same way as the cross-polarization spectra, except that a 120 μs delay was inserted before data acquisition to allow the signal from N–H to decay. The resulting spectra are due to nitrogens which do not bear protons.

Rate and $\Delta H^{\ddagger}$ determinations for the reaction

$$(Me_2AlNH_2)_3 \rightarrow (MeAlNH)_n + CH_4 \quad (2)$$

were performed in the following three ways:

(1) A few milligrams of $(Me_2AlNH_2)_3$ was placed in the bottom of a 5 mm NMR tube (below the receiver coil), and the capped tube was removed from the glovebox and inserted into the probe of the NMR instrument, which had been equilibrated at the temperature of interest. After a 7 minute wait to allow thermal equilibration, the ^1H $CH_4(g)$ signal above the sample was monitored over time. The increase was fitted to the equation

$$Y = Y_0 + (Y_f - Y_0)(1 - \exp(-kt)) \quad (3)$$

where Y is the signal height, Y_0 the initial signal, Y_f the final

(16) Auld, J.; Houlton, D. J.; Jones, A. C.; Rushworth, S. A.; Critchlow, G. W. *J. Mater. Chem.* **1994**, *4*, 1245 (and references therein). Manasevit, H. H.; Erdmann, F. M.; Simpson, W. I. *J. Electrochem. Soc.: Solid State Sci.* **1971**, *188*, 1864.
(17) Work of E. Wiberg, reported in: Bahr, G. In *Inorganic Chemistry, Part 2*; Klemm, W., Ed.; FIAT Review of WWII German Science; 1948; Vol. 24, p 155.
(18) Interrante, L. V.; Lee, W.; McConnell, M.; Lewis, N.; Hall, E. *J. Electrochem. Soc.* **1989**, *136*, 472.
(19) Sauls, F. C.; Czekaj, C. L.; Interrante, L. V. *Inorg. Chem.* **1990**, *29*, 4688.
(20) Mole, T.; Jeffery, E. A. *Organoaluminum Compounds*; Elsevier; Amsterdam, 1972; p 229.
(21) Lappert, M. F.; Power, P. P.; Sanger, A. R.; Srivastava, R. C. *Metal and Metalloid Amides*; Wiley: New York, 1980; p 99.
(22) Eisch, J. J. Aluminum. In *Comprehensive Organometallic Chemistry*; Wilkinson, G., Ed.; Pergamon: Oxford, England, 1982; Vol. 1, p 555.
(23) Taylor, M. J. Aluminum and Gallium. In *Comprehensive Organometallic Chemistry*; Wilkinson, G., Ed.; Pergamon: Oxford, England, 1987; Vol. 3, p 107.
(24) Cesari, M.; Cucinella, S. Aluminum–Nitrogen Rings and Cages. In *The Chemistry of Inorganic Homo- and Heterocycles*; Haiduc, I., Sowerby, D. B., Eds.; Academic Press: London, 1987; p 167.
(25) Interrante, L. V.; Sigel, G. A.; Garbauskas, M.; Hejna, C.; Slack, G. A. *Inorg. Chem.* **1989**, *28*, 252.
(26) Interrante, L. V.; Carpenter, L. E.; Whitmarsh, C.; Slack, G. A. *Mater. Res. Soc. Symp. Proc.* **1986**, *73*, 359.
(27) Sauls, F. C.; Interrante, L. V.; Shaikh, S. N.; Carpenter, L. E. *Inorg. Synth.*, in press.
(28) Sauls, F. C.; Interrante, L. V.; Jiang, Z. *Inorg. Chem.* **1990**, *29*, 2989.
(29) Amato, C. C.; Hudson, J. V.; Interrante, L. V. *Mater. Res. Soc. Symp. Proc.* **1991**, *204*, 135.
(30) van Geet, A. *Anal. Chem.* **1968**, *40*, 2227.

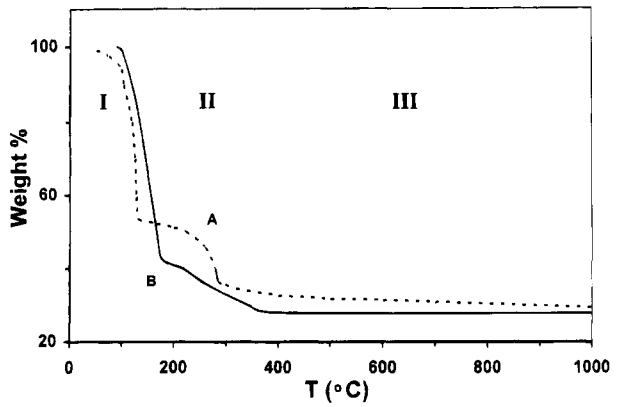

Figure 1. TGA of (Et_2AlNH_2) under nitrogen (B, solid line) and ammonia (A, broken line).

signal, and k the rate constant. Repetition of this process at various temperatures followed by a plot of ln k vs $1/T$ gave $\Delta H^{\ddagger}$.

(2) An NMR tube containing a solution of $(Me_2AlNH_2)_3$ in deuterated tetrahydronaphthalene ($C_{10}D_{12}$) was placed in the NMR probe and allowed to thermally equilibrate. The methyl ^1H NMR signal of the starting material was measured over time. A plot of ln(peak height) vs time was linear, indicating approximately first-order decomposition (slope = $-k$). Repetition of this process at various temperatures followed by a plot of ln k vs $1/T$ gave $\Delta H^{\ddagger}$. Attempts to repeat this process in the presence of ammonia gave an increase in the rate of decomposition, but the difficulty in keeping the ammonia concentration constant led to wide scatter in the results.

(3) Using the DSC-7, $(Me_2AlNH_2)_3$ was analyzed in a sealed stainless steel cell (loaded in the glovebox) by heating from ambient temperature at 2 °C/min. Activation energy and reaction order were determined from the relationship[31]

$$k = (dH/dt)(m_0/H_0)m^x \quad (4)$$

where k = rate constant, dH/dt = heat flow, m_0 = original sample mass, H_0 = total heat change, m = mass of unreacted sample, and x = reaction order. A plot of ln k vs $1/T$ gave $\Delta H^{\ddagger}$.

BET measurements were made on a Digisorb 2500 using N_2 gas. Powder XRD was performed on an automated Phillips Model PW 1710 diffractometer with step size 0.02°; sample powders were held on glass microscope slides using hydrocarbon grease. GCMS was performed on a Hewlett-Packard Model 5870.

C, H, N, and Al determinations were performed by Galbraith Laboratories. Oxygen was determined by neutron activation at General Atomics Corp.

Results

Figure 1B shows the TGA curve for $(Et_2AlNH_2)_3$ under a nitrogen atmosphere. The TGA for $(Me_2AlNH_2)_3$ is similar, except that the temperature for each decomposition is slightly higher and there is a substantial weight loss prior to decomposition due to the higher volatility of the Me–amide.

The plot may be divided into three regions. In region I (up to ca. 150 °C) the principal reaction

$$(R_2AlNH_2)_3 \rightarrow (RAlNH)_n + RH \quad (5)$$

is taking place, based on elemental analysis of the resultant solid and the demonstration that the evolved gas is chiefly the RH alkane. For this reaction, DSC yields a ΔH of −71 kJ/mol of methane for the methyl compound, and −83 kJ/mol of ethane for the ethyl. The smaller exotherm, higher decomposition temperatures, and generally slower reactions of the methyl derivatives are attributable to the greater strength of Al–methyl bonds compared to those with other alkyl groups.[32]

In region II (150–350 °C), also based on the elemental composition of the solid and analysis of the gas, the principal reaction is

$$(RAlNH)_n \rightarrow AlN + RH \quad (6)$$

where the "AlN" is an amorphous solid that contains residual carbon and hydrogen. The ΔH for this process is approximately zero for both the methyl and ethyl compounds.

In region III (ca. 350–1000 °C) the residual hydrogen is lost and the AlN assumes a partially crystalline form (vide infra) and, in the absence of NH_3, retains a significant amount (ca. 2.5%) of carbon.

The theoretical ceramic yield for the pyrolysis of $(Et_2AlNH_2)_3$ to AlN is 40.5%; however, the observed ceramic yield was only 28% because some $(Et_2AlNH_2)_3$ vaporizes during pyrolysis.

Under pyrolysis in ammonia the residual carbon content is markedly reduced, compared to pyrolysis under nitrogen. This is presumably due to NH_3-assisted elimination of hydrocarbons in the early stages of the pyrolysis (vide infra). The theoretical weight composition of AlN is Al 65.82%, N 34.12%. A sample of $(Et_2AlNH_2)_3$ pyrolyzed to 1000 °C under nitrogen contained 2.53% C. An identical sample pyrolyzed under ammonia contained 0.21% C. After further heating under nitrogen at 1600 °C for 4 h, this sample contained 65.82% Al, 34.03% N, 0.06% C, and less than 0.3% O.

On the basis of the TGA results, samples of $(Et_2AlNH_2)_3$ were pyrolyzed in ammonia or nitrogen atmospheres to 200, 350, 500, 800, and 1000 °C. The 200 °C sample represents $(EtAlNH)_n$ slightly converted to AlN. The others represent various stages of conversion of $(EtAlNH)_n$ to nanocrystalline "AlN".

Region I. $(R_2AlNH_2)_3$ to $(RAlNH)_n$ by RH Loss (up to 150 °C). The loss of methane from $(Me_2AlNH_2)_3$ was followed by ^1H NMR spectroscopy (Figure 2). The rightmost peak is due to the methyl hydrogens in $(Me_2AlNH_2)_3$. Peak A is the first product peak to appear. It rapidly increases in intensity and then virtually disappears as decomposition proceeds and other product peaks appear downfield. These multiple product peaks ($-0.65 > \delta > -0.85$) first increase in intensity then slowly decrease as the product becomes insoluble. We attribute these product peaks to Me–AlN_3 in a variety of environments.

^{27}Al NMR of $(Et_2AlNH_2)_3$ pyrolyzed to 200 °C under ammonia shows a broad set of peaks centered near 100 ppm (Figure 3), in general agreement with earlier results.[33] We attribute these resonances to nonequivalent AlN_3C tetrahedra in the $(EtAlNH)_n$. This is consistent with the range of nonequivalent methyl environments found in the ^1H NMR when $(MeAlNH)_n$ is formed. The observed relatively broad line widths

(31) Wendtlandt, W. W. *Thermal Methods of Analysis*, 3rd ed.; Wiley: New York, 1980; p 282.

(32) Skinner, H. A. *Adv. Organomet. Chem.* **1964**, *2*, 49.

(33) Baker, R. T.; Bolt, J. D.; Reddy, G. S.; Roe, D. C.; Staley, R. H.; Tebbe, F. N.; Vega, A. *J. Mater. Res. Soc. Symp. Proc.* **1988**, *108*, 337.

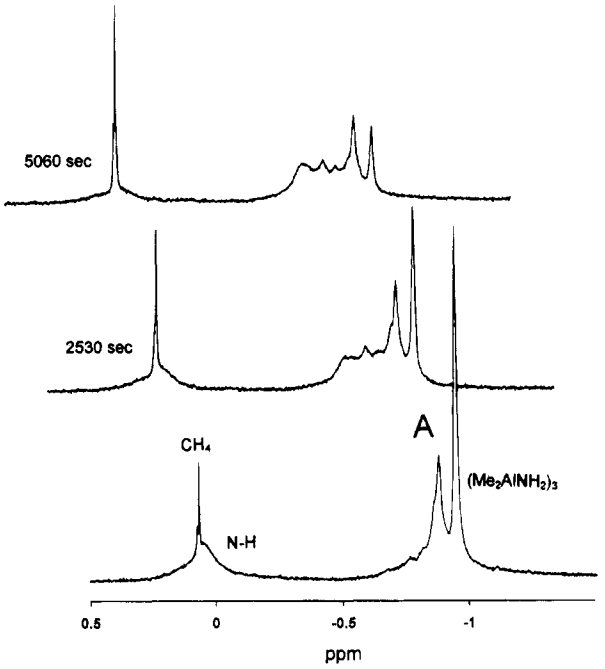

Figure 2. Decomposition of $(Me_2AlNH_2)_3$ in tetrahydronaphthalene-d_{12} at 126.2 °C. The lowest scan was obtained 7 min after the sample was inserted into the probe.

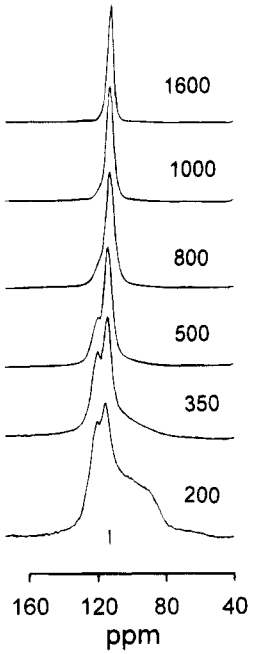

Figure 3. ^{27}Al MAS NMR of $(Et_2AlNH_2)_3$ pyrolyzed under ammonia for 4 h at the temperatures indicated. The vertical line indicates the position of the AlN resonance.

are presumably due to the residual second-order quadrupolar effects of ^{27}Al in the asymmetric environment and the range of chemical shifts associated with the nonequivalent environments. Superimposed on this is a relatively narrow peak associated with AlN_4 tetrahedra near 114 ppm, indicating partial conversion of the amide to AlN.[34]

The ^{15}N NMR spectrum (Bloch decays) for the ^{15}N-enriched $(Et_2AlNH_2)_3$ pyrolyzed under ammonia at 200 °C shows a single peak at ca. 35 ppm. This peak is

(34) Dupree, M.; Lewis, H.; Smith, M. E. *J. Appl. Cryst.* **1988**, *21*, 109.

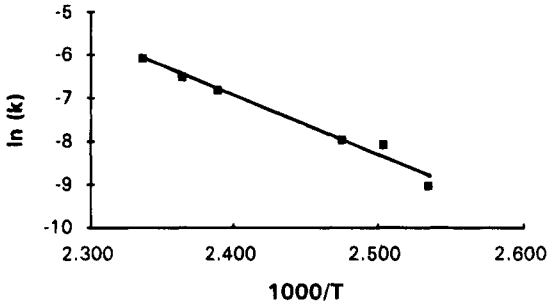

Figure 4. Determination of $\Delta H^{\ddagger}$ for $(Me_2AlNH_2)_3 \rightarrow (MeAlNH)_n + CH_4$ in $C_{10}D_{12}$.

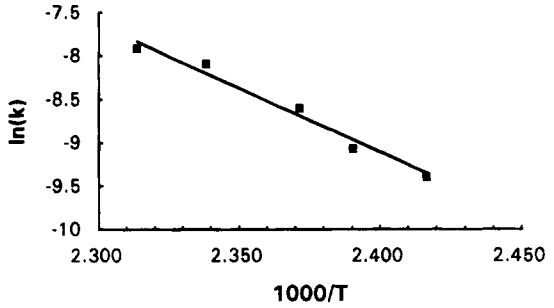

Figure 5. Determination of $\Delta H^{\ddagger}$ for $(Me_2AlNH_2)_3 \rightarrow (MeAlNH)_n + CH_4$ (neat).

attributed to N in H_xNAl_y environments.[33] Observation of this resonance required recycle delays on the order of 100 s, implying a relaxation time of roughly this magnitude. This relatively short relaxation time for nitrogen (vide infra for samples pyrolyzed to $T > 350$ °C) is probably due to a combination of (a) efficient dipolar relaxation due to the adjacent Al present in AlN_3C tetrahedra (cf. supra) on the ^{15}N relaxation; (b) dipolar-induced relaxation from the protons; (c) motion.

$\Delta H^{\ddagger}$ and the reaction order for this decomposition were examined by three methods: (1) Decomposition of neat $(Me_2AlNH_2)_3$ in the NMR tube followed first-order kinetics with $\Delta H^{\ddagger}$ 126 ± 11 kJ/mol (Figure 4). (2) Decomposition of the solution of $(Me_2AlNH_2)_3$ in deuterated tetrahydronaphthalene in the NMR was also first order with $\Delta H^{\ddagger}$ of 116 ± 9 kJ/mol (Figure 5). (3) The DSC method gave an activation energy of 130 kJ/mol and an order of 1.2.

The initial rapid weight loss shown in the TGA curves for $(Et_2AlNH_2)_3$ under both N_2 and NH_3 (Figure 1B,A) is due to the loss of ethane from the amide. It is evident that ammonia speeds this loss of ethane, as the steep portion extends to ca. 180 °C under nitrogen, but ends at only ca. 130 °C under ammonia. The slope is also greater under ammonia, implying a greater rate of alkane loss. The results of the solution kinetics study also support this conclusion for the methyl compound. Ammonia also increases the amount of carbon removed during pyrolysis. Intermediate A in Figure 2 does not appear when the decomposition takes place in the presence of ammonia.

Region II. $(RAlNH)_n$ to AlN by RH Loss (ca. 150–350 °C). Comparison of Figure 1A and 1B in the region 150–350 °C shows that, in both cases, the weight loss shows an obvious change in slope in the vicinity of 120–170 °C, which we associate with the onset of the loss of the second mole of ethane from the amide (the "imide" to AlN conversion). In contrast to the conversion under ammonia, the "plateau" associated with this ethane loss

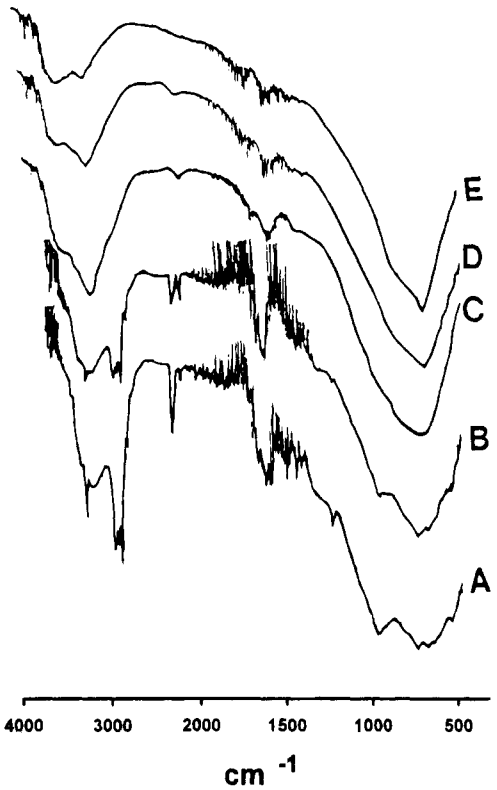

Figure 6. FTIR spectra of $(Et_2AlNH_2)_3$ pyrolyzed under ammonia at 200 (A), 350 (B), 500 (C), 800 (D), and 1000 °C (E). Samples A–D were heated 4 h, E for 6 h.

in the case of the pyrolysis under nitrogen is not well defined, and this region of relatively more rapid weight loss extends to a considerably higher temperature. The lack of a plateau after the first ethane loss implies that there is no clean separation of the first and second ethane loss steps when the pyrolysis is conducted in the absence of ammonia. Ammonia clearly improves the degree of separation of these two steps, although there is obviously still an appreciable overlap in the two processes.

Pyrolysis of a small amount of $(EtAlNH)_n$ in a sealed, evacuated tube followed by GC/MS analysis of the gases evolved showed principally the expected ethane, along with some methane, propane, butane, and pentane. The last four are probably due to the presence of the corresponding alkyl groups in the initial triethyl aluminum, which contains ca. 5% of related alkylaluminum compounds. A significant amount of ethylene and small amounts of propene and butene probably arose from a β-elimination mechanism.[35,36] CO_2 and H_2O were present along with trace amounts of acetaldehyde, propionaldehyde, ethylamine, and CO. A GC analysis showed that the principal pyrolysis products (ethane, ethylene, *n*-butane) were the same whether the pyrolysis was carried out under nitrogen or ammonia.

The IR spectra of the 200 and 350 °C intermediate solid products of the $(Et_2AlNH_2)_3$ pyrolysis under ammonia (Figure 6A,B) show the loss of the alkyl groups (C–H stretching peak, just below 3000 cm^{-1}). There are also small peaks at 2255 cm^{-1} (just below the artifact due to atmospheric CO_2) and 3162 cm^{-1} which

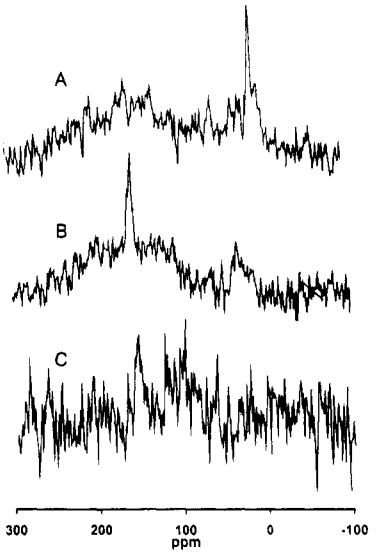

Figure 7. Single-pulse $^{13}C\{^1H\}$ MAS solid-state spectra for $(Et_2AlNH_2)_3$ pyrolyzed for 4 h at 200 (A), 350 (B), and 500 °C (C).

are attributed to[37] C≡C and ≡C–H formed by initial H loss from the ethyl groups.

The ^{13}C NMR spectrum of $(Et_2AlNH_2)_3$ in solution shows peaks at 9.1 and 0.8 ppm, corresponding to the CH_3 and CH_2 groups. The solid-state ^{13}C NMR spectrum (Figure 7) for the 200 °C sample (ammonia pyrolysis) contains a substantial peak near 10 ppm, confirming the continued presence of alkyl carbon.[38] The small peak near 60 ppm may reflect the low concentration of C≡C.[38] At 350 °C, the alkyl peak (36 ppm) has become less intense, broader, and shifted somewhat downfield. Less easily explained is a substantial peak near 160 ppm. This is in the carbonyl region of the spectrum and may represent C=O formed by reaction with traces of oxygen present. The traces of aldehydes and CO found by mass spectrometry lend some support to this. By 500 °C this peak has practically disappeared.

Region III. AlN Crystallization. Since no peaks appear in the XRD for samples heated to 800 °C (under ammonia or nitrogen), after the alkane molecules are lost by approximately 350 °C the AlN formed is essentially amorphous. Further heating to and beyond 1000 °C leads to increased crystallization and a reduction in surface area. Comparison of line widths in Figure 8B,C shows the increase of crystallinity with heating beyond 1000 °C. The peaks are those characteristic of 2H–AlN. Comparison of Figure 8A,B shows that heating in ammonia also increases the degree of crystallization, compared with heating in nitrogen. This suggests that ammonia facilitates the rearrangement of the Al–N bonds necessary for crystal growth. This improved crystallinity may also be related to the reduction in carbon content in the 1000 °C product obtained under ammonia pyrolysis.

The TGA for the pyrolysis under nitrogen is essentially flat after the loss of the last alkane at ca. 350 °C (Figure 1B); however, that under ammonia shows a slow decrease in the same region. From the FTIR of samples pyrolyzed under ammonia (Figure 6C) we

(35) Smith, W. L.; Wartik, T. J. *Inorg. Nucl. Chem.* **1967**, *29*, 1629.
(36) Boyd, D. C.; Haasch, R. T.; Mantell, D. R.; Schulze, R. K.; Evans, J. F.; Gladfelter, W. L. *Chem. Mater.* **1989**, *1*, 119.
(37) Silverstein, R. M.; Bassler, R. C.; Morrill, T. C. *Spectrometric Identification of Organic Compounds*, 5th ed.; Wiley: New York, 1991; p 107.
(38) Reference 37, p 236.

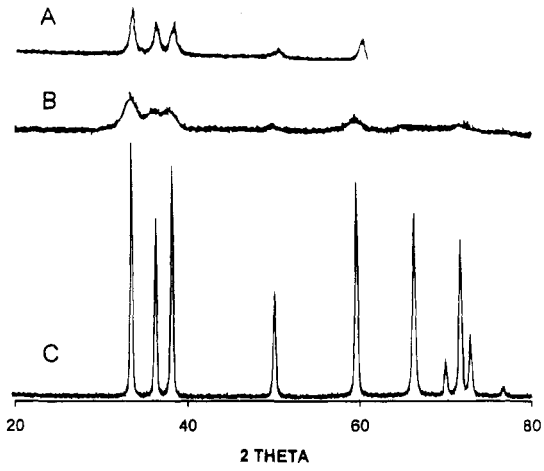

Figure 8. XRD of $(Et_2AlNH_2)_3$ pyrolysis product after heating 6 hours at (A) 1000 °C in ammonia, (B) 1000 °C in nitrogen, and (C) 1600 °C in nitrogen.

observe that at T > 350 °C all C−H groups have disappeared (disappearance of the peak just below 3000 cm^{-1}), yet there remains a substantial N−H peak near 3300 cm^{-1} (the absence of splitting of this peak implies[39] that it is N−H, not NH_2). Samples pyrolyzed under nitrogen do not show this N−H absorption. This N−H peak gradually decreases with increasing pyrolysis temperature. We attribute both the slope of the DSC plot and the N−H peak to the retention of ammonia as $Al-NH_{x(x<3)}$ by the lattice after the loss of alkane. Slow loss of NH_3 over the range 350−1000 °C would explain these results.

The results of BET surface area measurements also show substantial differences for the "AlN" obtained under nitrogen and ammonia. $(Et_2AlNH_2)_3$ pyrolyzed under nitrogen to 1000 °C had <0.1 m^2/g, while pyrolysis under ammonia gave 59.7 m^2/g. Incorporation of ammonia prior to the last alkane loss leads to the formation of a structure retaining excess NH_3; when the ammonia is later lost, the remaining solid has a high degree of porosity.

^{27}Al MAS NMR spectra (Figure 3) show that at 350 °C the peaks due to AlN_3C (100 ppm) have largely disappeared. In addition to the major peak near 114 ppm there is also a downfield shoulder which we associate with other environments such as AlN_3NH, AlN_3N:, or strained regions. This assignment of the shoulder is supported by its disappearance in parallel both with the N−H peak in the ^{15}N NMR spectrum (45 ppm, vide infra) and with the N−H stretching peak in the IR. The narrowness of these peaks implies that the ^{27}Al are now in a more symmetrical AlN_4 environment, with reduced quadrupolar broadening.[40] The spectra of samples heated to higher temperatures show that the shoulder disappears and the peak narrows, suggesting that these altered environments are converted to normal AlN_4 by ammonia loss and recrystallization.

Attempts to acquire ^{15}N NMR (Bloch decay) spectra for enriched samples pyrolyzed to 350 °C or higher were unsuccessful, even with recycle times of 900 s. The relaxation time of nitrogen in the AlN lattice is therefore long. This is consistent with conversion of these AlN_3C to AlN_4 environments.

(39) Reference 37, p 123.
(40) Bloembergen, N. *Nuclear Magnetic Relaxation*; Benjamin: New York, 1961; p 118.

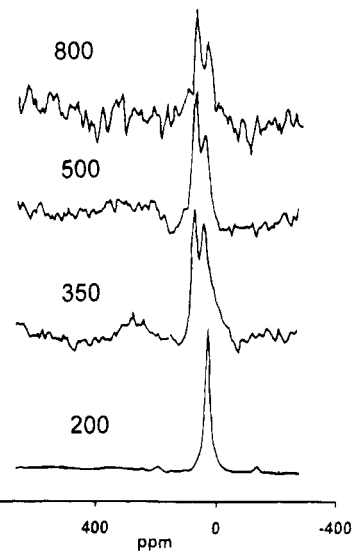

Figure 9. ^{15}N CPMAS spectra for enriched $(Et_2AlNH_2)_3$ pyrolyzed 4 h under ammonia at the temperatures (°C) indicated.

Table 1. Coarsening of AlN

	BET surface area (m^2/g)	
hours at 1605 °C	under N_2	under Kr
0	39.3	39.3
1	21.43	20.77
2	16.31	15.66
4	13.30	12.45
16	10.15	8.46

The evidence for retention of N−H by the lattice suggested that ^{15}N CPMAS be attempted for the enriched 200−1600 °C samples (Figure 9). Spectral intensity is due to ^{15}N near to protons; isolated $^{15}NAl_4$ are unobserved. The 200 °C sample showed a peak near 35 ppm as expected from the Bloch decay result. Each of the spectra of the samples pyrolyzed 350−800 °C showed two peaks, near 45 and near 80 ppm. In each, the 45 ppm peak was somewhat less intense than the 80 ppm peak. As the pyrolysis temperature increased, the peaks became less intense, roughly in parallel. CPMAS spectra were not observed for samples pyrolyzed to 1000 °C.

We attribute the 45 ppm peak to Al_3N-H in the lattice, and that at 80 ppm to Al_4N nearby. The loss of ammonia from the lattice as pyrolysis temperature increased would explain their parallel disappearance. The assignments are supported by the results of interrupted decoupling experiments, which remove peaks due to ^{15}N which is strongly dipolar coupled to protons. These spectra show a very weak peak near 30 ppm for the 200 °C sample, and only the 80 ppm peak for the 350−800 °C samples. By 800 °C this peak is very weak as well, as expected from the CP results.

Table 1 shows the results of coarsening AlN at 1605 °C under nitrogen or krypton atmosphere. The greater effect of Kr suggests that even at this temperature elemental nitrogen does not significantly open the AlN structure, in contrast with ammonia.

Discussion

$(R_2AlNH_2)_3$ to $(RAlNH)_n$. In Scheme 1 we suggest that the mechanism for the loss of alkane from $(R_2AlNH_2)_3$ begins with the opening of a ring, yielding

Scheme 1. Proposed Mechanism for Imide Formation

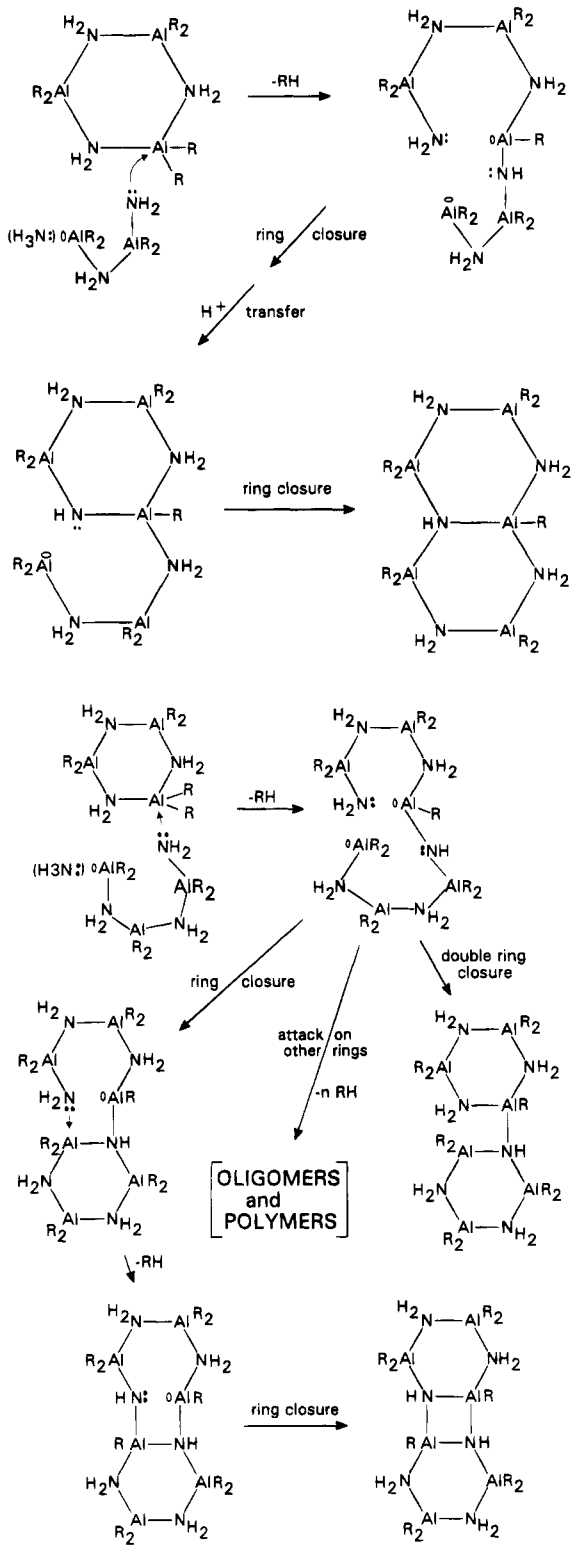

a terminal $:NH_2-$. This nitrogen may then attack an AlR_2 on a neighboring ring, leading to alkane loss and ring opening. The rings may then reclose in one of several possible ways or attack other rings, leading to a variety of linked ring and oligomeric/polymeric products. This is likely to be accompanied by relatively rapid proton transfer between N centers of different basicity within these intermediates. The rate-determining step in this process is probably the heterolytic ring-opening reaction that frees a N lone pair (along with an electron deficient Al center). The activation energy of ca. 123 kJ/mol (which is in the range of the previously determined values for the Al←N coordinate-covalent bond energy[28]) and the apparent first order of the decomposition are in agreement with this hypothesis.

Further ring openings and alkane losses lead to a variety of linked and fused rings. Mass spectroscopic evidence for some of these has been obtained in gas-phase studies of the $(Me_2AlNH_2)_3$ decomposition.[41] These higher oligomers then presumably condense further via similar RH elimination reactions to produce extended polymeric species based on fused four- and six-membered $(AlN)_{2,3}$ rings. This structure may be viewed as the "imide", "RAlNH", with pendant $-NH_2$ and $-AlR_2$ groups.

As the condensation continues and more rings are added, the structure becomes increasingly rigid. This will restrict the mobility of the $:NX_2-$ and AlY_2- groups, thus limiting their ability to effect continued condensation.

Ammonia is known to add reversibly to these ring compounds[19,42] and to accelerate the ring equilibration process. These adducts, probably ring opened dimeric and trimeric forms of the (R_2AlNH_2), may react by the proposed mechanism without difficulty (the effect of added ammonia is shown in parentheses in Scheme 1). Thus $\Delta H^{\ddagger}$ should be smaller and the reaction faster in the presence of NH_3. The resultant NH_3 adducts also should provide a convenient source of H for transfer to adjacent R groups, enabling their removal as RH. Thus, the resultant AlN will contain less elemental carbon and crystallization will be facilitated.

The ability of NH_3 to add to these rings will also affect the structure of the product "imide". In its absence there will probably be strained regions formed, as well as regions where there are two adjacent Al−R groups or N−H, instead of the Al−R and N−H pair required for alkane elimination. The presence of ammonia will allow the rings to open and reclose in a less-strained arrangement. Thus the local environments will be more variable in the "imide" formed under nitrogen than that formed under ammonia.

We speculate that peak A in Figure 2 is due to the terminal Me_2Al- groups formed by heterolytic ring opening. In the presence of ammonia, such groups would not be formed, explaining the absence of this peak in the samples heated under ammonia.

Bolt and Tebbe[43,44] have reported that loss of alkane from the trimer in the presence of excess trialkylaluminum forms a viscous and soluble polymer, in contrast to the insoluble imide otherwise produced. This viscous product is irreversibly solidified by removal of the trialkylaluminum by distillation or by the addition of ammonia. Trialkylaluminum would coordinate to the nitrogen lone pairs formed in Scheme 1, preventing final closure of the rings. This would result in flexible links between the rings rather than their fusion and a more soluble and tractable product. Removal of the trialkylaluminum would result in irreversible closure.

(41) Amato, C. C.; Hudson, J. V.; Interrante, L. V. *Mater. Res. Soc. Proc.* **1993**, *282*, 611.
(42) Alford, K. J.; Gosling, K.; Smith, J. D. *J. Chem. Soc., Dalton Trans.* **1972**, 2203.
(43) Tebbe, F. N.; Bolt, J. D. *Mater. Res. Soc. Symp. Proc.* **1988**, *108*, 337.
(44) Bolt, J. D.; Tebbe, F. N. *Adv. Ceram.* **1989**, *26*, 69.

$(RAlNH)_n$ to AlN. The lack of a plateau in the TGA and presence of some AlN_4 tetrahedra after pyrolysis at 200 °C (under ammonia) strongly suggest that the final alkane loss overlaps the terminal stages of the "amide" to "imide" conversion. There is thus no clear separation of these steps and no clearly distinguishable "imide" species. The wide temperature range over which the final alkane is lost from the amide under nitrogen is probably due to the range of local environments present. This further implies that even prolonged heating at, e.g., 200 °C, where some AlN_4 tetrahedra are formed, is unlikely to completely remove the alkyl groups.

The final product also contains a significant amount of residual carbon. As decomposition proceeds, areas will form where the residual Al−R are not adjacent to the remaining N−H. Alkyl group loss must then occur by either β-hydrogen elimination or homolytic Al−C bond cleavage, producing olefinic or free-radical species, respectively, which could in turn subsequently pyrolyze to form carbon. Alternatively, these Al−C groups may gradually lose hydrogen as temperatures increase, leaving carbidic carbon.

These processes which compete with alkane loss are likely to become of increasing importance in the latter stages of the conversion. This may account for the lack of a distinct exotherm or endotherm for the last step.

Ammonia affects the chemical conversion in several ways (Figure 1A): (1) the process is completed over a narrower range of temperatures; (2) there is a long tail of continued weight loss extending to much higher temperatures; (3) the final product contains much less carbon when the pyrolysis is done under ammonia.

We attribute each of these effects to the ability of ammonia to open the aluminum−nitrogen rings and thereby become incorporated into the structure (Scheme 2). Reaction with ammonia opens a ring producing an $-Y_2Al-NH_3$ and $:NX_2-$. The $:NX_2-$ may then open an Al−N bond in a neighboring ring, effectively propagating through the structure. A proton could also be transferred to the terminal nitrogen. Continuation of these processes would distribute the three N−H hydrogens and the $:NX_2-$ throughout the structure.

Scheme 2. Effects of Ammonia on the AlN Lattice

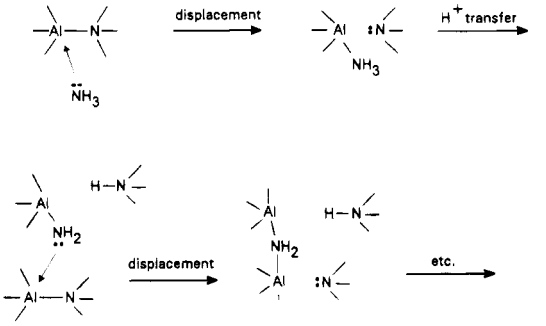

This process would be expected to have several consequences for alkane loss. The ability to open rings will allow the strained regions to relax toward more stable configurations. This will facilitate the elimination of RH and result in a more clearly defined conversion of the imide to AlN. Moreover, the increase in N−H hydrogens in the solid will make it more probable that a residual alkyl group will have a neighboring N−H, thus decreasing the probability of its pyrolysis to carbon.

Recrystallization. The ammonia remaining incorporated into the AlN after the loss of the last alkane has several important effects on the crystallization. The resulting structure will have a coordination number of four for aluminum and on average somewhat less than four for nitrogen. In addition, some of the nitrogen atoms will have terminal hydrogen or lone pairs instead of being bonded to aluminum. This will result in a less rigid and more open structure. The lone pairs on the nitrogens can effectively travel through the solid, allowing the local structure to relax to a more ordered (and more stable) form. The virtual absence of residual carbon at the AlN grain boundaries will also facilitate crystallization by not impeding the growth of the AlN crystallites.

Acknowledgment. This work was supported by NSF Grant CHE-9114181 to F.C.S. and CHE-9202973 to L.V.I.

CM9500566